Supporting Information

[60]Fullerene-Porphyrin [*n*]Pseudorotaxanes: Self-Assembly, Photophysics and Third-order NLO responses

Luka Đorđević, Tomas Marangoni, Federica De Leo, Irene Papagiannouli, Panagiotis Aloukos, Stelios Couris, Eleonora Pavoni, Filippo Monti, Nicola Armaroli,* Maurizio Prato and Davide Bonifazi**

Table of Contents

S1	Instruments and Materials	1
S2	Synthetic Procedures	3
S3	Characterization ^{1}H and ^{13}C NMR spectra	9
S4	Diffusion Measurements	13
S5	MALDI-TOF Spectra	18
S6	Photophysics	20
S7	Z-Scan Measurements	21
S8	Molecular Modelling	26
S9	References	28

S8 Instruments and Materials

Compounds were fully characterized (^{1}H and ^{13}C NMR, ESI-MS, IR, m.p.).

NMR spectra were obtained on a *Varian Gemini* 200 spectrometer (200 MHz ^{1}H and 50 MHz ^{13}C) or on a *Varian* Inova spectrometer (500 MHz ^{1}H and 125 MHz ^{13}C). Chemical shifts are reported in ppm using the solvent residual signal as an internal reference ($CDCl_3$: δ_H = 7.26 ppm, δ_C = 77.23 ppm). The resonance multiplicity is described as *s* (singlet), *d* (doublet), *t* (triplet), *q* (quartet), *dd* (doublet of doublets), *m* (multiplet), *bs* (broad singlet). The Self-diffusion coefficient evaluations were carried out using Varian INOVA (500 MHz) NMR spectrometer equipped with Performa II-Z gradient coils (Varian).

Mass spectrometry Electrospray Ionization (ESI, 5600 eV) mass analysis was performed on a *Perkin-Elmer* API1 by Dr. Fabio Holland.

HR-MALDI-MS mass spectrometry (LC-MS) Mass spectrometry was performed by the *Centre de spectrométrie de masse at the Université de Mons in Belgium*. MALDI-MS were recorded using a *Waters QToF Premier mass spectrometer* equipped with a nitrogen laser, operating at 337 nm with a maximum output of 500 mW delivered to the sample in 4 ns pulses at 20 Hz repeating rate. Time-of-flight analyses were performed in the reflectron mode at a resolution of about 10,000.

All spectroscopic measurements in solution were carried out in fluorimetric 10.00 mm path cuvettes using spectroscopic grade solvents. UV–Vis–NIR absorption spectra in solution were recorded with a Perkin-Elmer Lambda 950 spectrophotometer. All emission spectra were obtained using an Edinburgh FLS920 spectrometer equipped with a Peltier-cooled Hamamatsu R928 photomultiplier tube (PMT, sensitive in the 185–850 nm range) for UV-Vis emission spectra. On the other hand, a Hamamatsu R5509-72 supercooled photomultiplier tube (operating at 193K and sensitive in the 500–1700 nm range) was used for recording NIR luminescence spectra. An Edinburgh Xe 900 (400 W) Xenon arc lamp was used as continuous excitation source for all steady-state emission spectra.

Photoluminescence quantum yields in solution (Φ) were obtained from corrected spectra on a wavelength scale (nm) and measured according to the approach described by Demas and Crosby[1] using an air-equilibrated $[Ru(bpy)_3][Cl]_2$ water solution as standard (Φ = 2.8%).[2]

Emission lifetimes in the UV–Vis region were measured by an IBH single photon counting spectrometer equipped with pulsed NanoLED excitation sources (λ_{ex} = 331 and 465 nm; pulse width 0.3 ns) and a red-sensitive (185–850 nm) Hamamatsu R-3237--01 PMT. NIR time-resolved measurements were carried out with the same single-photon counting technique by means of the Edinburgh FLS920 spectrometer using a laser diode as the excitation source (λ_{exc} = 407 nm; 200 ps time resolution after deconvolution) with the above-

mentioned Hamamatsu R5509-72 PMT as detector. Analysis of the luminescence decay profiles against time was accomplished with the software provided by the manufacturer of each instrument.

IR spectra (KBR) were recorded on a Perkin Elmer 2000 spectrometer by Paolo De Baseggio.

Melting Points (m.p.) were measured on a Büchi SMP-20.

Z-scan was performed employing a mode-locked Nd:YAG laser (YG900, Quantel).

Chemicals were purchased from Sigma Aldrich, TCI, and Acros and used as received. Solvents were purchased from VWR, Sigma Aldrich and Acros, and deuterated solvents from Sigma Aldrich and Cambridge Isotope Laboratories. General solvents such as Toluene, THF, and Et_3N were distilled from Na, Na/benzophenone, and CaH_2 respectively. Thin layer chromatography (TLC) was conducted on pre-coated aluminum sheets with 0.20 mm Machevery-Nagel Alugram SIL G/UV254 with fluorescent indicator UV254. Column chromatography was carried out using Merck Gerduran silica gel 60 (particle size 40-63 μm).

S2 Synthetic Procedures

Compounds **3**[3],**4**[4] and **5**[5] were synthetized and characterized according to literature procedures.

5,10,15-Triphenyl-20-[(4-hydroxybenzyl)-succinyl-meth-3-yl-[6,7,9,10,12,13,20,21,23,24,26,27-dodecahydrodibenzo[b,n][1,4,7,10,13,16,19,22]octaoxacyclotetracosine]-porphyrin (1)

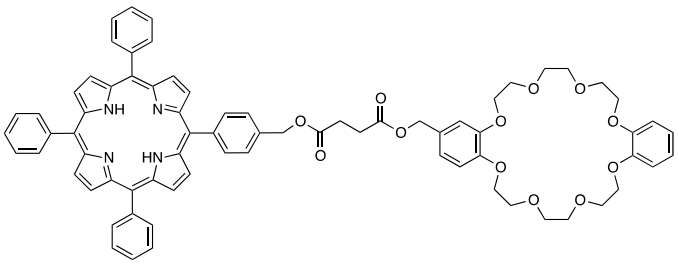

To a solution of **6** (75 mg, 0.130 mmol), **9** (40 mg, 0.062 mmol) and 4-DMAP (16 mg, 0.130 mmol) in CH_2Cl_2 (7 ml) was added EDC · HCl (25 mg, 0.130 mmol) at 0 ˚C under Ar. The reaction was left to warm up to room temperature and was left stirring overnight under Ar. The reaction mixture was diluted with CH_2Cl_2 (30 ml) and the organic layer was washed with 0.1 M aq. HCl (2 x 40 ml), sat. aq. K_2CO_3 solution (2 x 40 ml) and H_2O (40 ml), dried (Na_2SO_4) and eliminated under vacuum. The mixture was purified by column chromatography (eluent: $CHCl_3$) to obtain **1** as a deep purple solid (50 mg, 67% yield). δ_H (500 MHz; $CDCl_3$; 298 K): 8.85 (s, 8H), 8.23-8.21 (m, 8H), 7.77-7.75 (m, 11H), 6.93-6.81 (m, 7H), 5.49 (s, 2H), 5.10 (s, 2H), 4.18-4.06 (m, 8H), 3.86-3.81 (m, 8H), 3.75 (s, 8H), 2.89-2.81 (m, 4H), -2.77 (s, 2H); δ_C (125 MHz; $CDCl_3$; 298 K): 172.52, 172.39, 149.25, 149.12, 142.36, 142.34, 135.51, 134.92, 134.77, 129.02, 127.95, 126.91, 126.62, 121.94, 121.61, 120.48, 120.42, 119.65, 114.61, 114.29, 113.87, 71.44, 71.41, 70.08, 70.02, 69.97, 69.70, 69.64, 69.59, 69.55, 66.85, 66.74, 29.58, 29.56. IR (cm^{-1}): ν 2918, 2889, 1730, 1630, 1597, 1408, 1380, 1347, 1258, 1219, 1147, 1125, 1058, 997, 969, 808, 741, 713. MS (5600 eV, ESI): found 1203.4 ($M - H^+$), $C_{74}H_{68}N_4O_{12}$ requires = 1204.48.

5,15-Biphenyl-15,20-Bis-[(4-hydroxybenzyl)-succinyl-meth-3-yl-6,7,9,10,12,13,20,21,23,24,26,27-dodecahydrodibenzo[b,n][1,4,7,10,13,16,19,22]octaoxacyclotetracosine]-porphyrin (2)

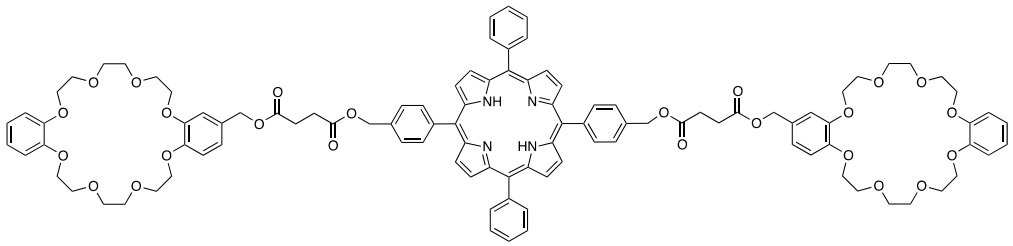

To a solution of **6** (90 mg, 0.156 mmol), **10** (25 mg, 0.037 mmol) and 4-DMAP (19 mg, 0.156 mmol) in CH_2Cl_2 (6 ml) was added EDC · HCl (30 mg, 0.156 mmol) at 0 ˚C under Ar. The reaction was left to warm up to room temperature and was left stirring overnight under Ar. The solvent was removed under vacuum and the residue was dissolved in CH_2Cl_2. The organic layer was washed with with 0.1 M aq. HCl (2 x 40 ml), sat. aq. K_2CO_3 solution (2 x 40 ml) and H_2O (40 ml), dried (Na_2SO_4) and eliminated under vacuum. The mixture was purified by column chromatography (eluent: $CHCl_3$, and then $CHCl_3$/MeOH 99:1) to obtain **2** as a deep purple solid (36 mg, 54% yield). δ_H (500 MHz; $CDCl_3$; 298 K): 8.85 (s, 8H), 8.23-8.19 (m, 8H), 7.78-7.71 (m, 10H), 6.95-6.81 (m, 14H), 5.49 (s, 4H), 5.11 (s, 4H), 4.17-4.06 (m, 16H), 3.88-3.81 (m, 16H), 3.76 (s, 16H), 2.90-2.81 (m, 8H), -2.78 (s, 2H); δ_C (125 MHz; $CDCl_3$; 298 K): 172.53, 172.40, 149.26, 149.14, 142.32, 142.30, 135.54, 134.92, 134.77, 129.02, 127.99, 126.93, 126.63, 121.94, 121.61, 120.48, 119.78, 114.60, 114.29, 113.87, 71.47, 71.44, 70.11, 70.04, 69.99, 69.72, 69.67, 69.60, 69.57, 66.86, 66.73, 29.58, 29.56. IR (cm^{-1}): ν 2917, 2889, 1732, 1599, 1505, 1452, 1385, 1352, 1256, 1127, 1044, 955, 802, 740. MS (5600 eV, ESI): found 1794.7 ($M - H^+$), $C_{104}H_{106}N_4O_{24}$ requires = 1795.7.

[(6,7,9,10,12,13,20,21,23,24,26,27-dodecahydrodibenzo[b,n][1,4,7,10,13,16,19,22]octaoxacyclotetracosine)-3-methoxy]-4-oxobutanoic acid (6)

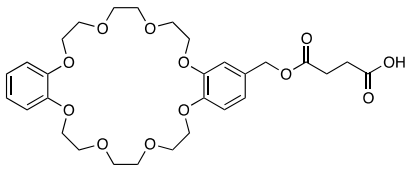

A pre-heated round-bottom flask (250 ml) was charged with **5** (200 mg, 0.418 mmol), succinic anhydride (44 mg, 0.443 mmol) and 4-DMAP (catalytic amount) in dry toluene (30 ml). The reaction was stirred at reflux overnight. The solution was left to cool to room temperature and the solvent was removed under vacuum. The crude product was precipitated from CH_2Cl_2 with CHX (2 x), pentane (2 x) and Et_2O (3 x) to obtain **6** as a white solid (205 mg, 85 % yield). m.p. 112-112.5 ˚C. δ_H (500 MHz; $CDCl_3$; 298 K): 6.88-6.82 (m, 7H), 5.03 (s, 2H), 4.21-4.09 (m, 8H), 3.92-3.87 (m, 8H), 3.82 (s, 8H), 2.64 (s, 4H). δ_C (125 MHz; $CDCl_3$; 298 K): 176.75, 172.24, 149.19, 149.09, 149.05, 129.01, 121.86, 121.62, 114.56, 114.26, 113.77, 71.45, 71.39, 70.11, 70.08, 70.01, 69.63, 69.56, 69.55, 66.72, 29.27, 29.01; IR (cm^{-1}): ν 2929, 2922, 1733, 1714, 1593, 1521, 1506, 1451, 1432, 1331, 1309, 1258, 1128, 1098, 1056, 941, 804. MS (5600 eV, ESI): found 577.2 ($M - H^+$), $C_{29}H_{38}O_{12}$ requires = 578.2.

5,10,15-Triphenyl-20-(4-methylbenzoate)-porphyrin (7)

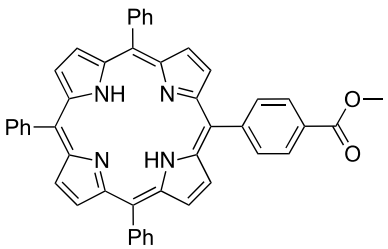

To a solution of benzaldehyde (0.22 ml, 2.19 mmol), methyl 4-formylbenzoate (330 mg, 2.19 mmol) and pyrrole (0.30 ml, 4.38 mmol) in 1.0 L of $CHCl_3$ was added $BF_3 \cdot OEt_2$ (0.36 ml) under Ar. The solution was stirred for 1 hour before adding Chloranil (400 mg, 0.33 mmol) and was left stirring for another hour. Finally, Et_3N

(0.28 ml) was added and all was stirred for 15 min. The solution was concentrated under reduced pressure and subjected to a preliminary CC (Pet. Et./CH_2Cl_2 1:1) to obtain a dark purple solid as a mixture of TPP and porphyrin esters. Compound **7** was purified by column chromatography as the second band (eluent: CHX/AcOEt from 95:5) and finally precipitated from CH_2Cl_2 with CHX (148 mg, 10% yield). m.p. > 300 °C. δ_H (200 MHz; $CDCl_3$; 298 K): 8.88 (m, 8H), 8.49-8.30 (dd, 4H, *j* = 26.8, 8.4 Hz), 8.27-8.17 (m, 6H), 7.81-7.73 (m, 9H), 4.12 (s, 3H), -2.78 (bs, 2H); δ_C (50 MHz; $CDCl_3$; 298 K): 167.48, 147.22, 142.20, 134.71, 131.37, 129.73, 128.09, 127.96, 126.89, 120.76, 120.56, 118.71, 52.67. IR (cm^{-1}): ν 2925, 2920, 1722, 1606, 1437, 1491, 1279, 1178, 1112, 965, 799, 726, 707. MS (5600 eV, ESI): found 673.4 ($M + H^+$), $C_{46}H_{32}N_4O_2$ requires = 672.3.

5,15-Biphenyl-15,20-Bis-(4-methylbenzoate)-porphyrin (8)

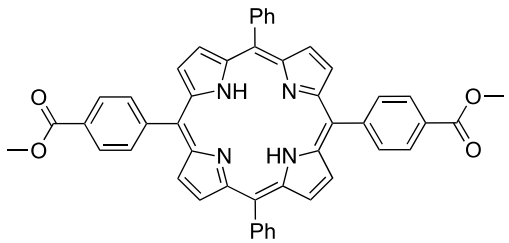

To a solution of benzaldehyde (0.22 ml, 2.19 mmol), methyl 4-formylbenzoate (330 mg, 2.19 mmol) and pyrrole (0.30 ml, 4.38 mmol) in 1.0 L of $CHCl_3$ was added $BF_3 \cdot OEt_2$ (0.36 ml) under Ar. The solution was stirred for 1 hour before adding Chloranil (400 mg, 0.33 mmol) and was left stirring for another hour. Finally, Et_3N (0.28 ml) was added and all was stirred for 15 min. The solution was concentrated under reduced pressure and subjected to a preliminary CC (Pet. Et./CH_2Cl_2 1:1) to obtain a dark purple solid as a mixture of TPP and porphyrin esters. Compound **8** was purified by column chromatography as the third band (eluent: CHX/AcOEt from 9:1) and finally precipitated from CH_2Cl_2 with CHX (144 mg, 9% yield). m.p. > 300 °C. δ_H (200 MHz; $CDCl_3$; 298 K): 8.85 (dd, 8H, *j* = 15.8, 5.0 Hz), 8.39 (dd, 8H, *j* = 28.6, 8.2 Hz), 8.25-8.19 (m, 4H), 7.81-7.73 (m, 6H), 4.12 (s, 6H), -2.78 (bs, 2H); δ_C (50 MHz; $CDCl_3$; 298 K): 167.43, 147.08, 142.10, 134.72, 131.69, 131.08, 130.85, 129.82, 128.13, 128.05, 126.94, 121.00, 120.80, 119.15, 118.96, 52.67. IR (cm^{-1}): ν

2926, 2921, 1724, 1604, 1435, 1489, 1275, 1175, 1112, 962, 802, 738. MS (5600 eV, ESI): found 731.4 ($M+H^+$), $C_{48}H_{34}N_4O_4$requires = 730.3.

5,10,15-Triphenyl-20-[(4-hydroxybenzyl)]-porphyrin (9)

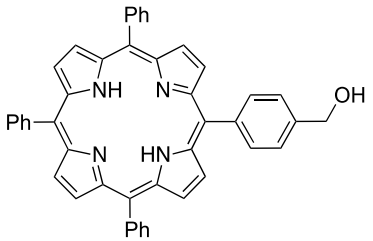

A solution of **7** (50 mg, 0.068 mmol) in dry THF (5 ml) was added dropwise to a suspension of $LiAlH_4$ (3 mg, 0.081 mmol) in dry THF (2 ml) at 0 ˚C under Ar. The reaction was left to stir for 30 min at room temperature before being quenched with EtOH (9 ml) and H_2O (1 ml). The mixture was diluted with CH_2Cl_2 (50 ml) and the organic layer was washed with H_2O (3 x 50 ml) and brine (30 ml), dried (Na_2SO_4) and concentrated. The crude product was purified by column chromatography (eluent: CHX/AcOEt 1:1), precipitated from THF with CHX to obtain **9** (38 mg, 81% yield). m.p. > 300 ˚C. δ_H (500 MHz; $CDCl_3$; 298 K): 8.89 (s, 8H), 8.26-8.21 (m, 8H), 7.80-7.72 (m, 11H), 5.02 (s, 2H), 1.96 (bs, 1H), -2.71 (s, 2H); δ_C (125 MHz; $CDCl_3$; 298 K): 142.38, 141.78, 140.46, 134.95, 134.76, 127.93, 126.90, 125.52, 120.40, 120.38, 119.96, 65.62. IR (cm^{-1}): ν 2919, 2911, 1631, 1468, 1440, 1257, 1118, 966, 1112, 965, 799, 736, 702. MS (5600 eV, ESI): found 643.3 ($M - H^+$), $C_{45}H_{32}N_4O$ requires = 644.3.

5,15-Biphenyl-15,20-Bis-(4-hydroxybenzyl)-porphyrin (10)

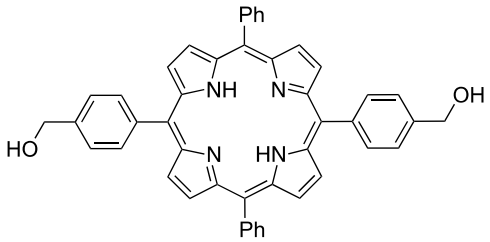

A solution of **8** (127 mg, 0.174 mmol) in dry THF (10 ml) was added dropwise to a suspension of $LiAlH_4$ (8 mg, 0.209 mmol) in dry THF (5 ml) at 0 ˚C under Ar. The reaction was left to stir for 30 min at room temperature before being quenched with EtOH (9 ml) and H_2O (1 ml). The mixture was diluted with $CHCl_3$ (75 ml) and the organic layer was washed with H_2O (3 x 70 ml) and brine (70 ml), dried (Na_2SO_4) and concentrated. The crude product was purified by column chromatography (eluent: CHX/AcOEt 5:5), precipitated from THF with CHX to obtain **10** (82 mg, 70% yield). m.p. > 300 ˚C. δ_H (500 MHz; $CDCl_3$; 298 K): 8.85 (s, 8H), 8.25-8.19 (m, 8H), 7.79-7.73 (m, 10H), 5.05 (s, 4H), 2.00 (bs, 2H), -2.76 (bs, 2H); δ_C (125 MHz; $CDCl_3$; 298 K): 142.35, 141.75, 140.47, 134.94, 134.76, 127.94, 126.91, 125.52, 120.43, 119.99, 65.61. IR (cm^{-1}): ν 2941, 2852, 1627, 1572, 1489, 1445, 1383, 1339, 1200, 1061, 965, 797, 713, 702. MS (5600 eV, ESI): found 675.4 ($M+H^+$), $C_{46}H_{34}N_4O_2$ requires = 674.8.

S3 Characterization ^{1}H and ^{13}C NMR spectra

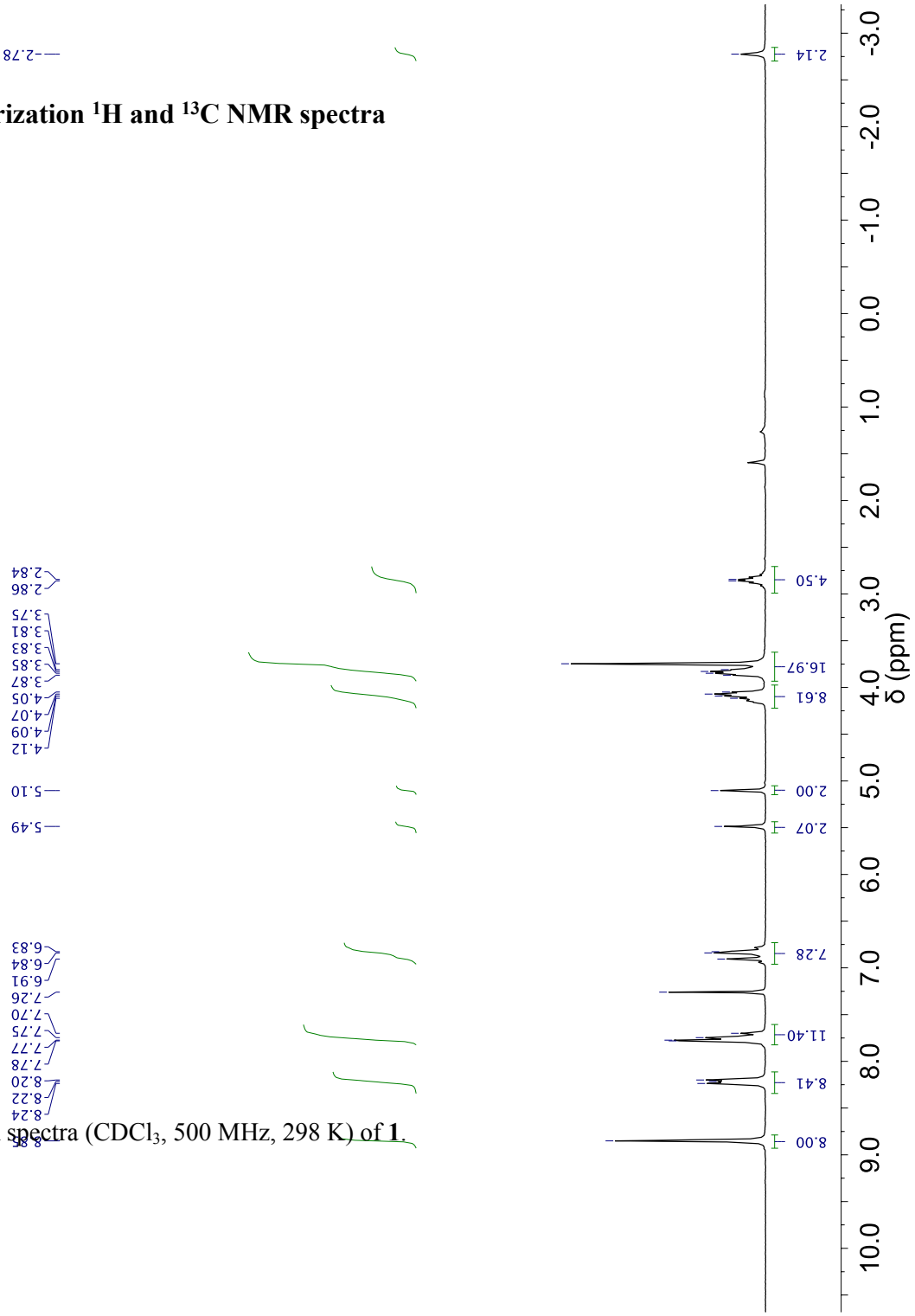

Figure S1. ^{1}H-NMR spectra ($CDCl_3$, 500 MHz, 298 K) of **1**.

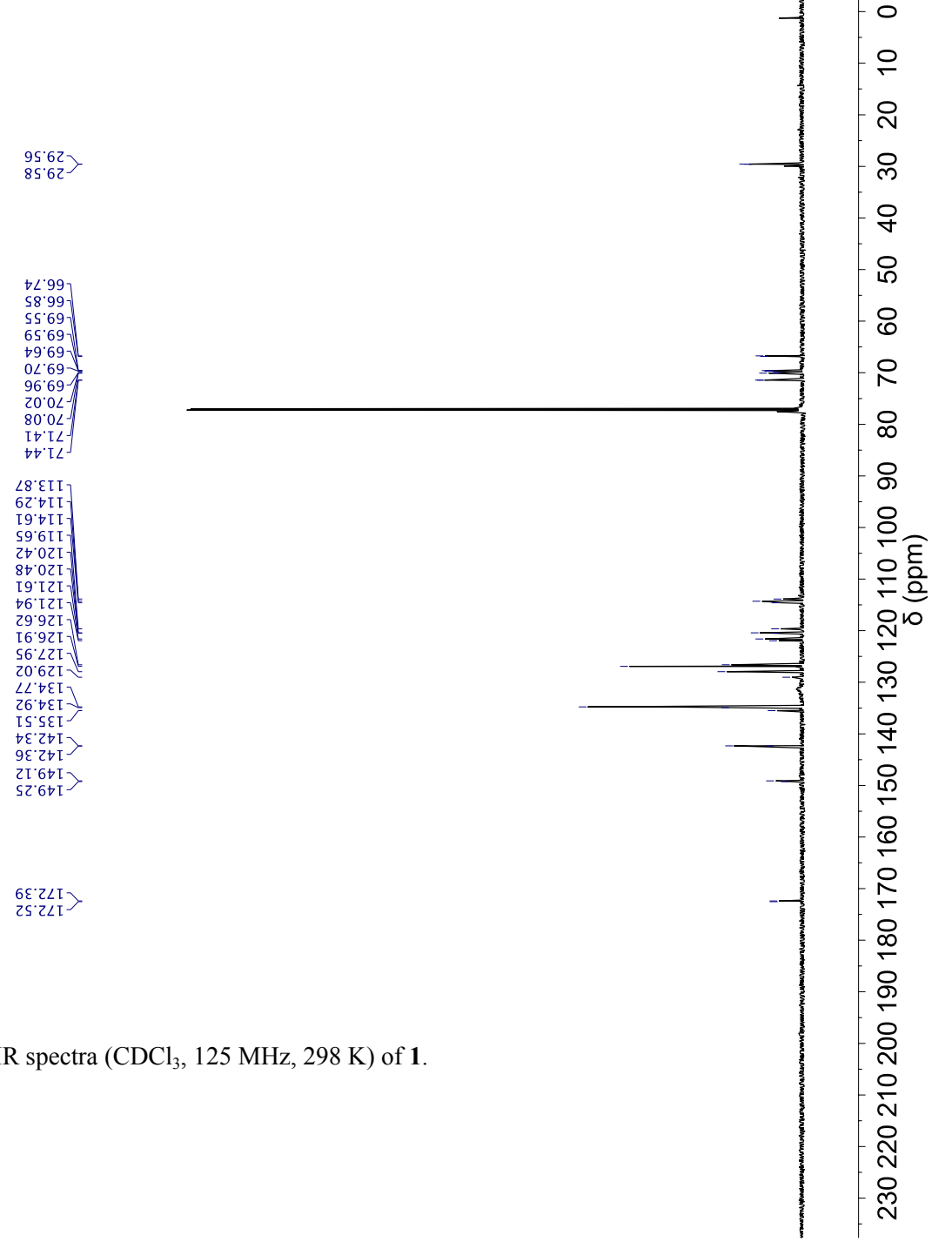

Figure S2. ^{13}C-NMR spectra ($CDCl_3$, 125 MHz, 298 K) of **1**.

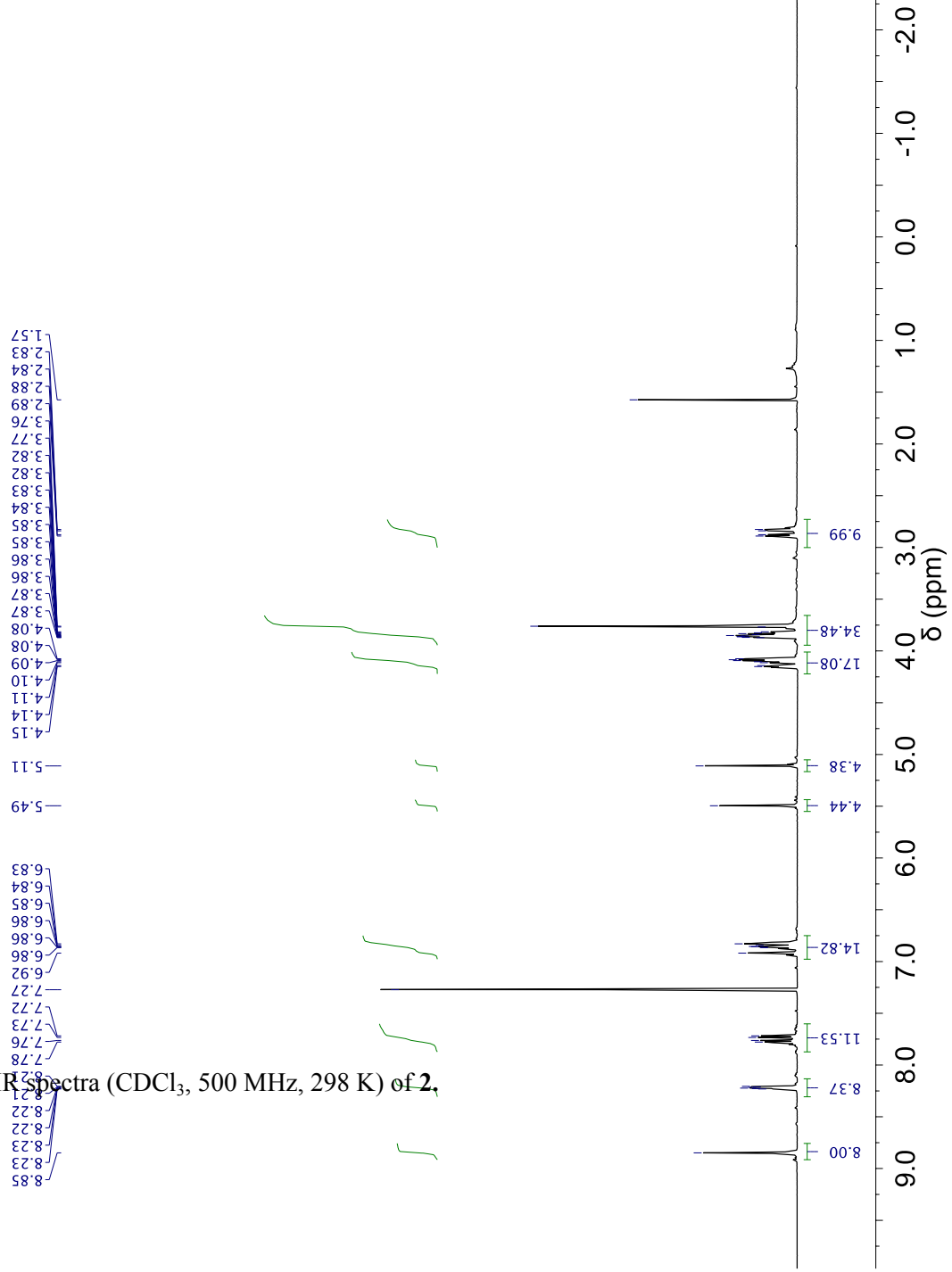

Figure S3. ^{1}H-NMR spectra ($CDCl_3$, 500 MHz, 298 K) of **2**.

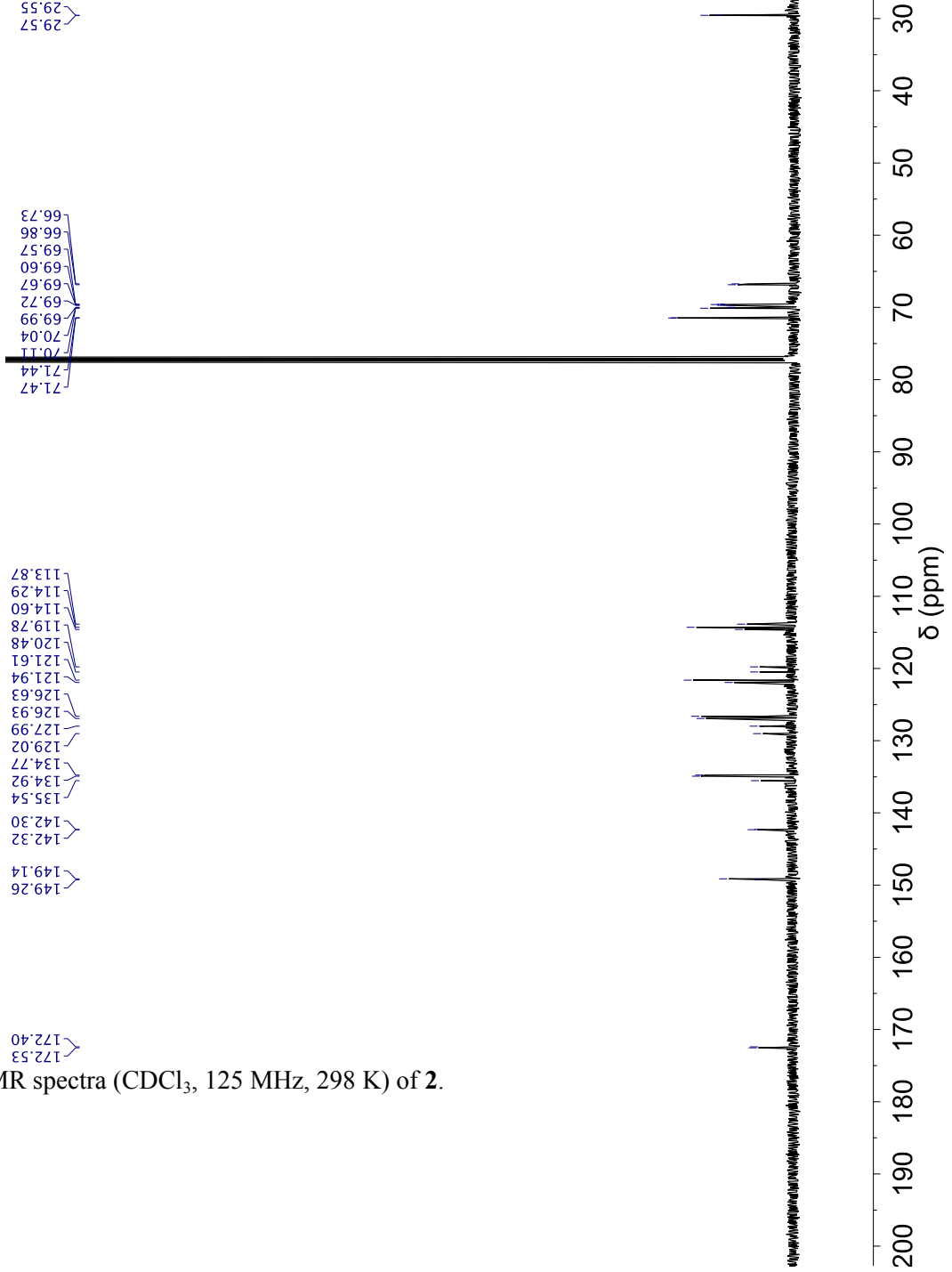

Figure S4. ^{13}C-NMR spectra ($CDCl_3$, 125 MHz, 298 K) of **2**.

5

S4 Diffusion Measurements

The gradient strength was calibrated with pure water (D = 2.229 x 10^{-9} m^2 s^{-1} at 298.2 K) and the maximum gradient strength was about 53 G·cm^{-1}. The Dbpsste_cc pulse sequence was used for the measurements of diffusion coefficient. Samples were weighted, transferred in 5-mm diameter NMR tubes and dissolved in the solvent ($CDCl_3$/CH_3CN 9:1, 500 µl) and then allowed to stand for at least one hour before starting measurements. Experiments were performed by keeping the z-gradient pulse length constant and gradually increasing the gradient strength in 15 steps. The gradient pulse length was 30 or 70 ms to measure the diffusion coefficient of all components. The diffusion coefficients (D) were obtained from the slope of the following equation:

$$ln\left(I_g/I_0\right) = -\left(\gamma^2\delta^2G^2(\Delta - \delta/3)\right)D$$

Where I_g and I_0 are intensities of the NMR signal in the presence and absence of field gradient pulses; γ is the gyromagnetic constant for ^1H; δ is the duration of the z-gradient pulse; G is the gradient strength; and Δ is the time interval between the gradient pulses (diffusion time). The D was obtained by fitting the experimental data (peak intensity with increasing gradient strength) by a multi-exponential function (least square fitting according the algorithm of Levenberg, 1944; Marquardt, 1963).

$$\sum_{k=1}^{N_e} \frac{I_k}{I_0} e^{-\left(\gamma^2\delta^2G^2(\Delta - \delta/3)\right)D^k}$$

Where I_k is the k^{th} pre-exponential factor and D^k is the k^{th} diffusion coefficient. The number of N_e of exponentials considered was that minimizing the product (N_e, □), where □ is the sum of squared differences referred to the equation fitting to experimental data.

Finally, D was placed in the Stokes-Einstein equation to obtain r_s, the hydrodynamic radius (or Stokes' radius) of the molecular species:

$$D = k_bT/6\pi\eta r_s$$

Where k_b is the Boltzmann constant, T is the absolute temperature and η is the viscosity of the medium. The viscosity of the solvent mixture was estimated using the Refutas equation.

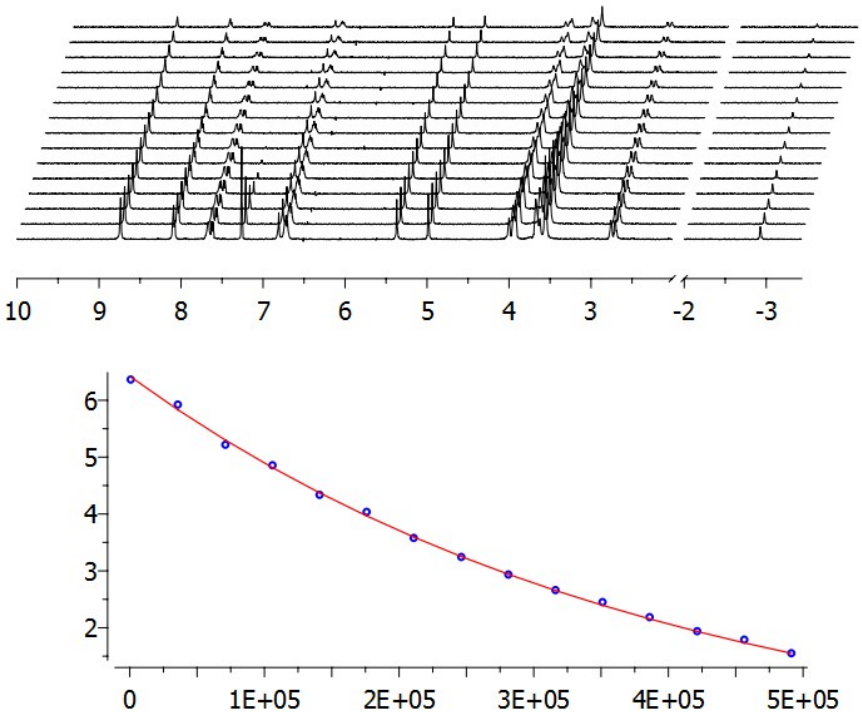

Figure S5. Diffusion signal decays for **1**.

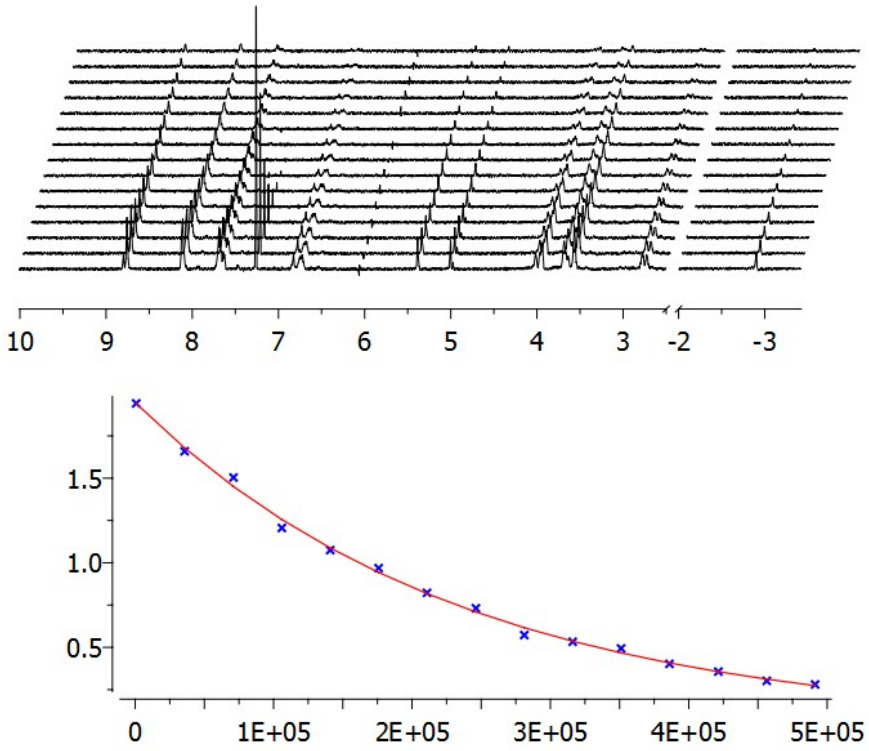

Figure S6. Diffusion signal decays for **2**.

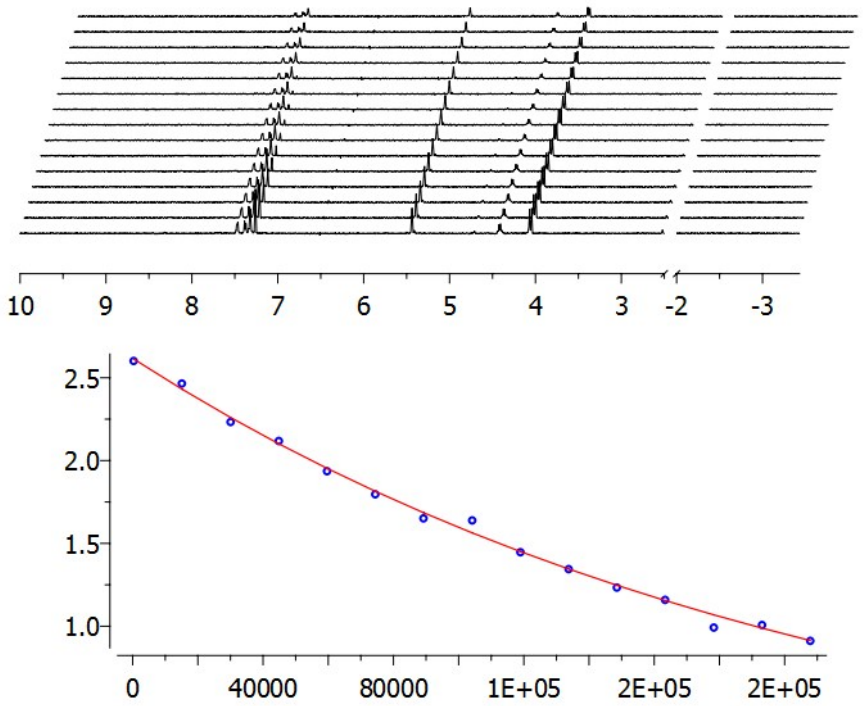

Figure S7. Diffusion signal decays for **3**.

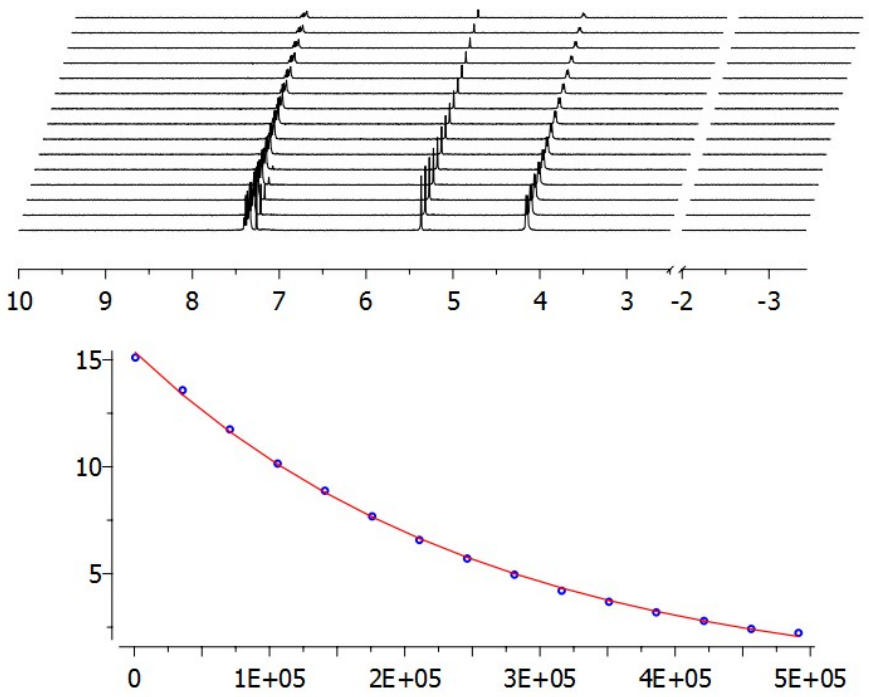

Figure S8. Diffusion signal decays for **4.**

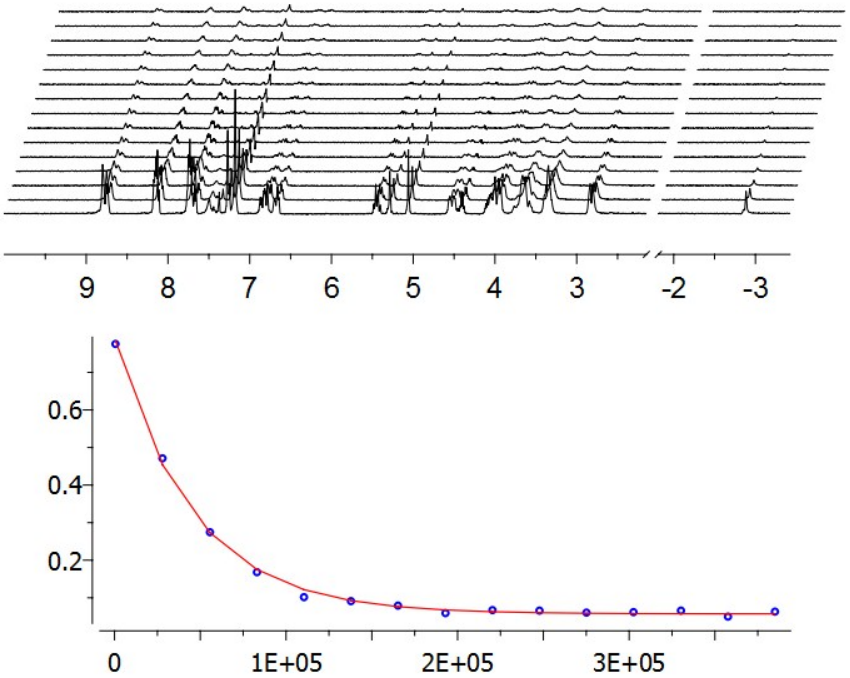

Figure S9. Diffusion signal decays for **1**·(**3**H_2)$_2$]·PF_6.

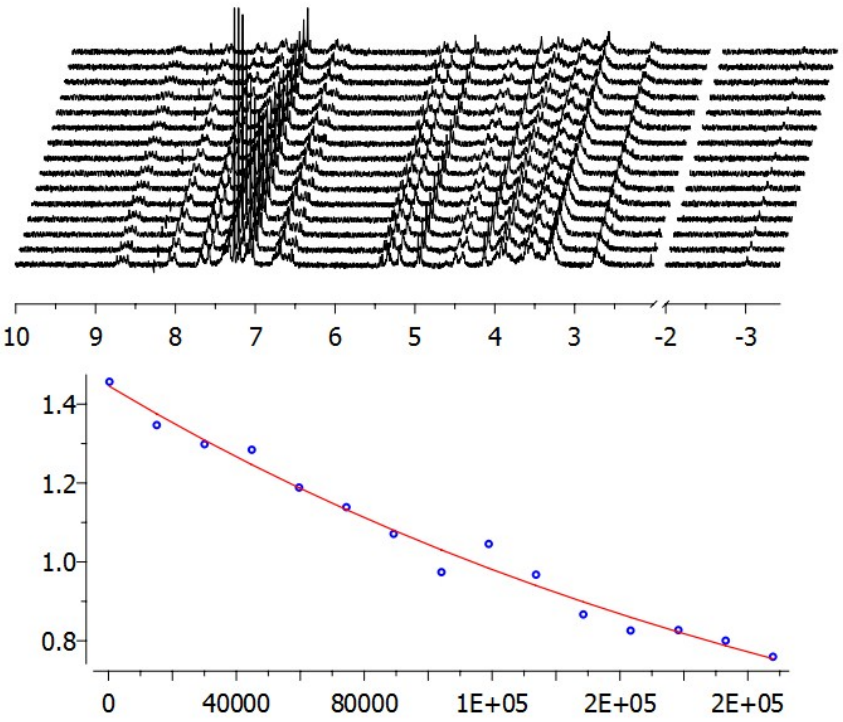

Figure S10. Diffusion signal decays for (**1**)$_2$·**4**H_4]·2PF_6

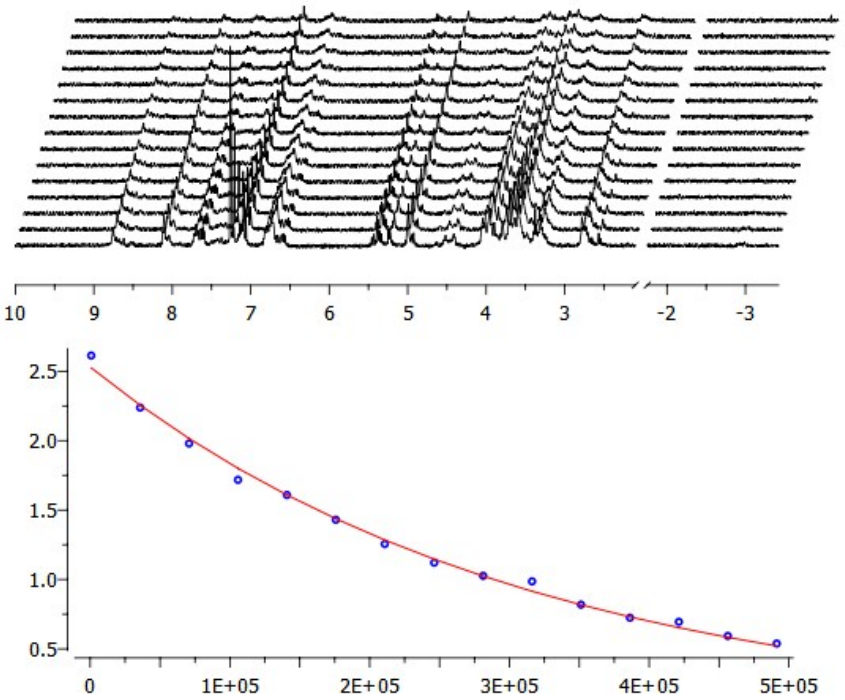

Figure S11. Diffusion signal decays for **2**·(**3**H_2)$_2$]·2PF_6.

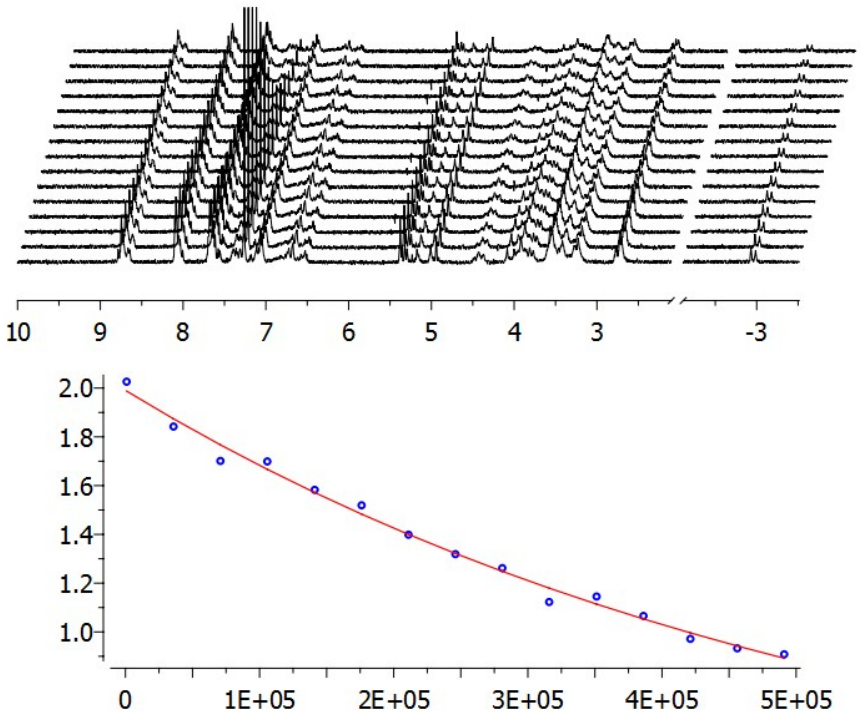

Figure S12. Diffusion signal decays for [**2**·**4**H_4]·2PF_6.

S5 MALDI-TOF Spectra

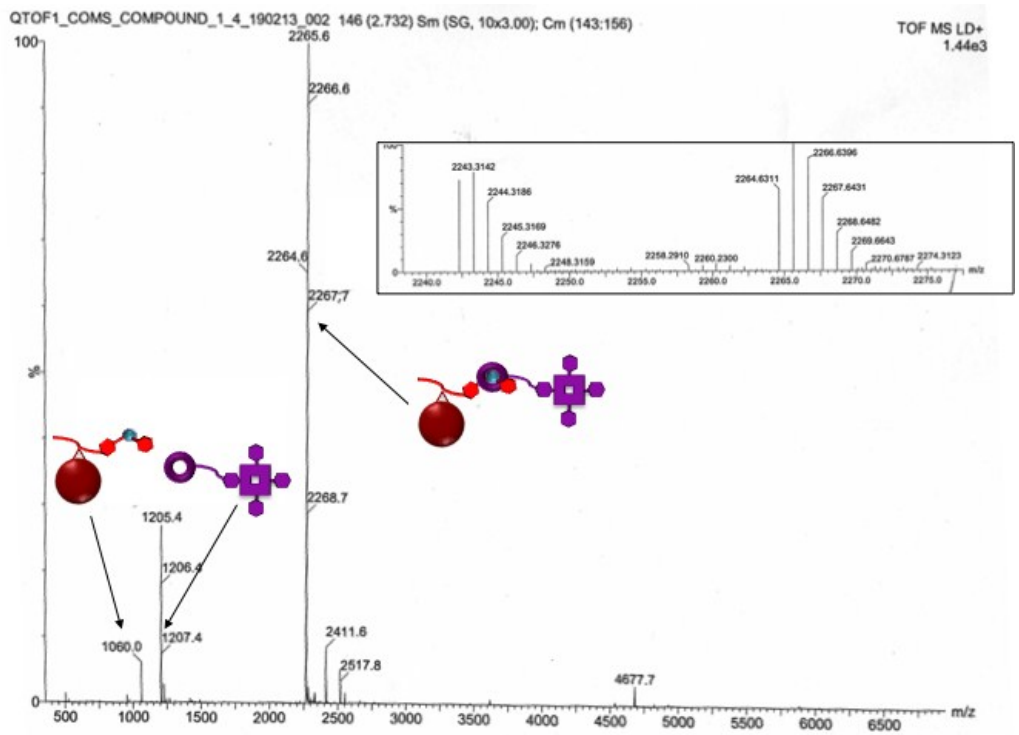

Figure S13. MALDI-TOF-MS spectra of $[\mathbf{1}\cdot\mathbf{3}H_2]\cdot PF_6$.

5

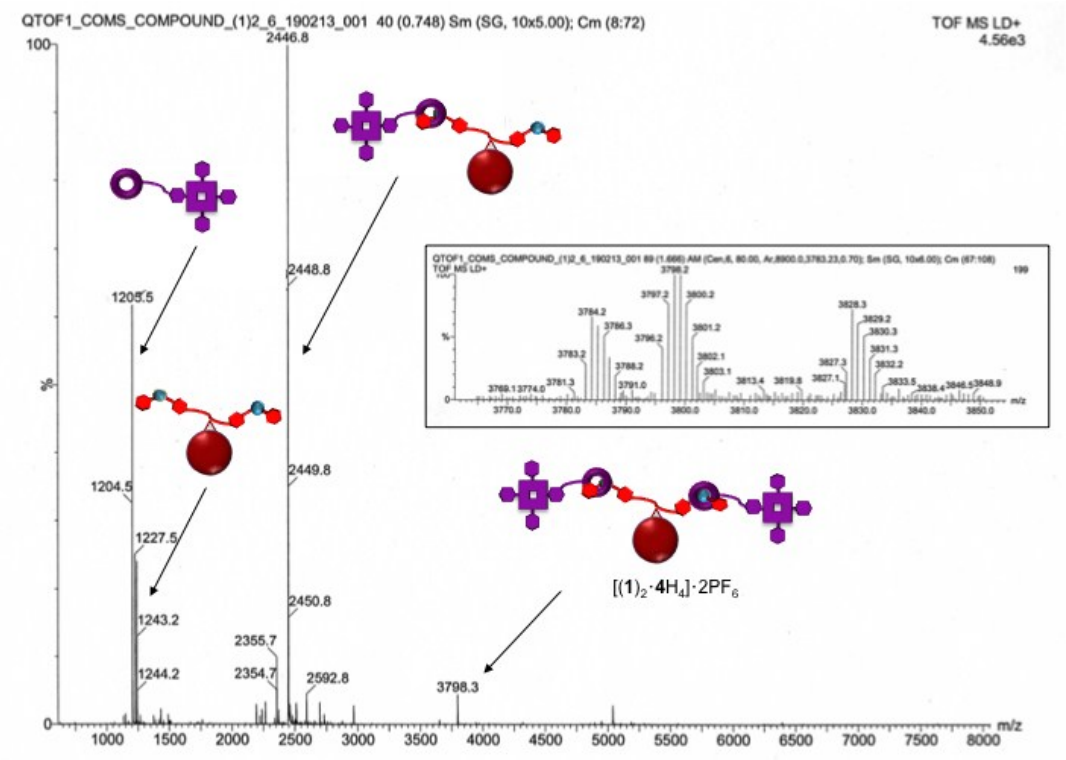

Figure S14. MALDI-TOF-MS spectra of $[(\mathbf{1})_2\cdot\mathbf{4}H_4]\cdot 2PF_6$.

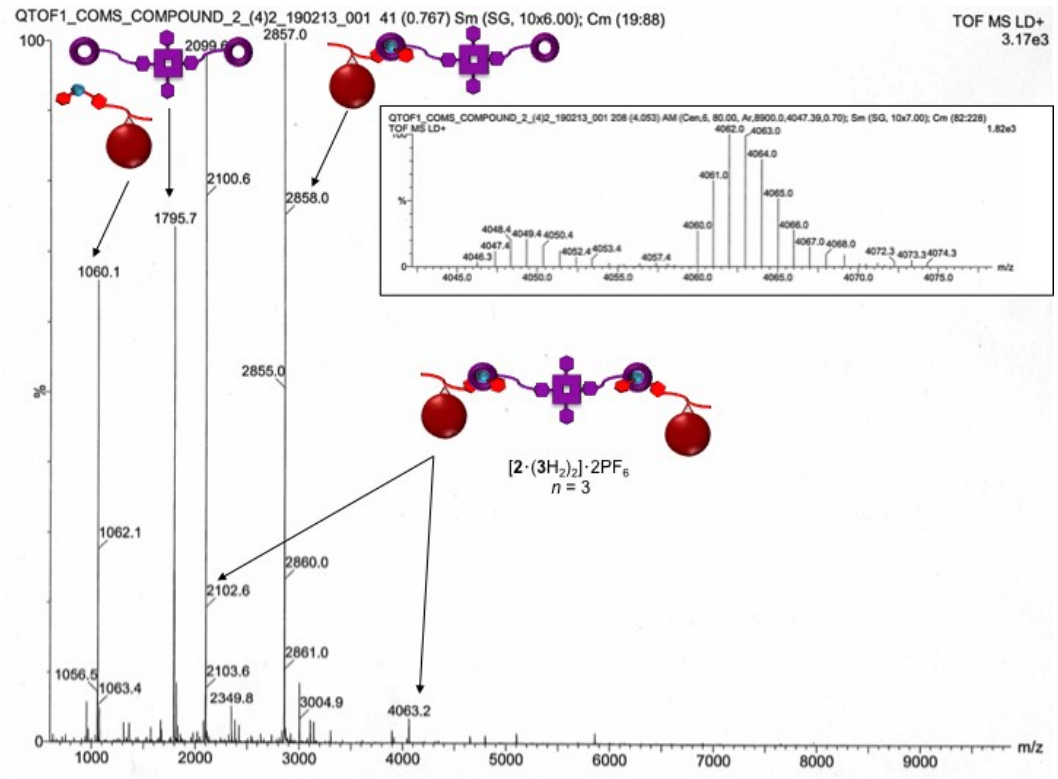

Figure S15. MALDI-TOF-MS spectra of $[\mathbf{2}\cdot(\mathbf{3}H_2)_2]\cdot 2PF_6$

5

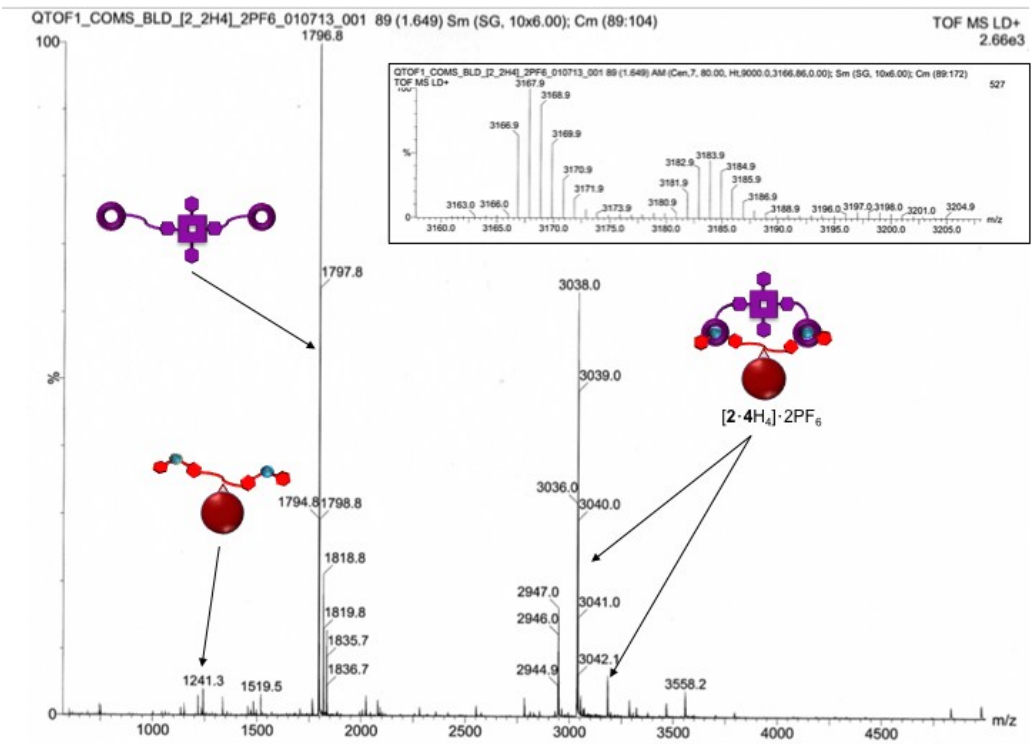

Figure S16. MALDI-TOF-MS spectra of $[\mathbf{2}\cdot\mathbf{4}H_4]\cdot 2PF_6$.

S6 Photophysics

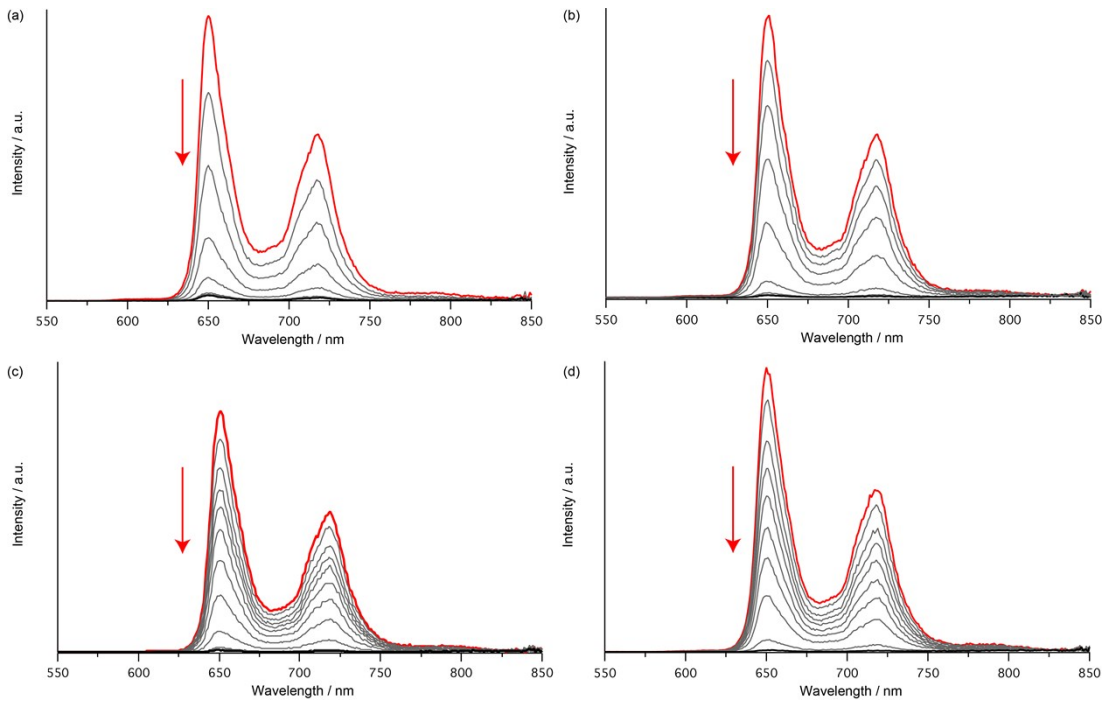

Figure S17. Luminescence spectra recorded at λ_{exc} = 420 nm in Et_2O/CH_3CN (98/2). Top: **1** (5.5 µM, red line) + 4 eq. of fullerene **3** (a) and **4** (b). Bottom: **2** (5.5 µM, red line) + 3 eq. of fullerene **3** (c) and **4** (d).

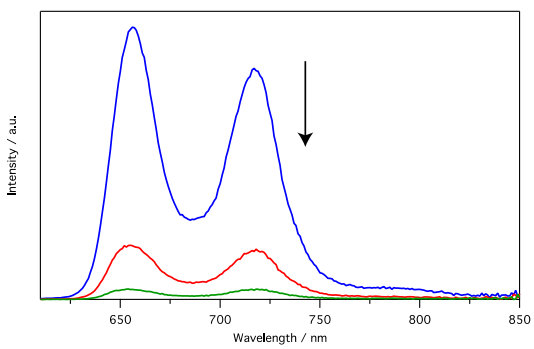

Figure S18. Emission spectra in CH_2Cl_2/CH_3CN (9:1) of **1** (0.25 mM) upon addition of 0.5 (blue), **1** (red), **2** (green) eq. of **3**. λ_{exc} 600 nm, NIR detector.

S7 Z-Scan Measurements

The nonlinear optical (NLO) parameters, i.e. the nonlinear absorption coefficient β and the nonlinear refractive index parameter γ' of the pseudorotaxane assemblies and all the individual molecular components (i.e., reference compounds), were determined using the Z-scan technique employing 532 nm, 35 ps laser pulses from a mode-locked Nd:YAG laser (Quantel YG900) operating at 10 Hz.[8] The laser beam was focused into the sample by means of a 20 cm focal length quartz lens and its energy was measured by an energy meter (Coherent J-10MB-LE). The samples were placed into 1mm thick quartz cells. The beam waist w_0 of the laser beam was determined using a CCD camera (Watec LCL-903HS) and was determined to be (17.4±0.5)μm at 532 nm. The transmitted through the sample laser light was detected by a photomultiplier (Hamamatsu R5108)and the electrical signal was further processed by a boxcar integrator (Stanford Research Systems, SR 250). The optical absorption spectra of the prepared solutions were measured on a Hitachi U-3010 spectrophotometer. So briefly, according to this technique, a sample is moving along the propagation direction of a focused laser beam (i.e., along the z-axis), thus experiencing different laser intensity at each z-position. Then, two types of transmission measurements are performed, the so-called "open-" and "closed-aperture" Z-scans. During the former transmission measurement, the transmitted laser light is measured just after the sample, as a function of the sample z-position. The nonlinear absorption coefficient β can be determined from the fitting of the "open-aperture" Z-scan transmission recording with the following equation:

$$T = \frac{1}{\sqrt{\pi}\left[\frac{\beta I_O L_{eff}}{1+z^2/z_o^2}\right]} \int_{-\infty}^{\infty} \ln\left[1+\frac{\beta I_O L_{eff}}{1+z^2/z_o^2}\exp(-t^2)\right] dt \qquad (1)$$

where $L_{eff} = \left[1-\exp(-a_0 L)\right]/a_0$ is the effective sample thickness, a_0 is the linear absorption coefficient, L is the sample length, z_0 is the Rayleigh length, z is the position of the sample and I_0 is the on the on-axis peak irradiance at the focal plane.

From the division of the "open-" by the "closed-aperture" Z-scan recordings, the "divided" Z-scan is obtained. In the case of low nonlinear absorption, the

nonlinear refractive index parameter γ' can be obtained from the "divided" Z-scan using the following relation:

$$\gamma' = \frac{\lambda \alpha_0}{1 - e^{-al}} \frac{\Delta T_{p-v}}{0.812 \pi I_0 (1 - S)^{0.25}} \quad (2)$$

where: $\Delta T_{p\text{-}v}$ is the difference of the normalized transmission between the peak and the valley of the "divided" Z-scan curve, $S = 1 - \exp(-2r_\alpha^2 / w_a^2)$ is the linear aperture transmission with r_α and w_α being the aperture radius and the beam radius on the aperture respectively and λ is the excitation laser wavelength.

The imaginary (Im $\chi^{(3)}$) and real (Re $\chi^{(3)}$) parts of the third-order susceptibility $\chi^{(3)}$ can be easily calculated from the following relations:

$$\mathrm{Re}\,\chi^{(3)}(esu) = \frac{c(m/s)\, n_0^2\, \gamma'(m^2/W)}{480\,\pi^2} \quad (3)$$

$$\mathrm{Im}\,\chi^{(3)}(esu) = \frac{c^2(m/\mathrm{s})^2\, n_0^2\, \beta(m/W)}{960\,\pi^2 \omega(\mathrm{s}^{-1})} \quad (4)$$

where c is the light velocity in m/s, ω is the excitation frequency in cycles/s and n_0 is the linear refractive index of the solvent.

Finally, the value of the second hyperpolarizability γ can be obtained from the following relation[4]:

$$\gamma = \chi^{(3)} / NL^4 \quad (5)$$

where N is the number of molecules per cm^3 and $L = (n_0^2 + 2)/3$ is the Lorenz-Lorentz local field correction factor. The second hyperpolarizability, γ, designates the magnitude of the nonlinearity per molecule, thus being a molecular constant.

For the determination of the NLO parameters measurements of the different molecular systems investigated in this work, several solutions with different concentrations were prepared for each molecule and were measured using different laser energies. In all cases, in order to check for contribution(s) of the neat solvents, i.e. CH_2Cl_2/CH_3CN and/or Et_3N, to the NLO response of the solutions, separate measurements of the solvents were performed under identical experimental conditions to those employed for the solutions. In all cases, it was confirmed that the solvents did not exhibit any contribution for the range of laser energies used for the

measurements of the solutions. Therefore, the shape of the Z-scan recording was reflecting straightforwardly the sign of the NLO response of the solute. In Figure 9, some representative "open-" and "divided-" Z-scans of solutions of the pseudorotaxanes in CH_2Cl_2/CH_3CN (9:1) are presented, obtained under 35 ps, 532 nm laser excitation. As shown, the "open-aperture" Z-scans of all pseudorotaxanes were found exhibiting reverse saturable absorption (RSA) behaviour, as indicated by the transmission minimum exhibited. From the fitting of these transmission recordings with equation (1), the nonlinear absorption coefficient β was determined and next the imaginary part of the third-order susceptibility was obtained from equation (4). In addition, the corresponding "divided" Z-scans were exhibiting a pre-focal transmission peak followed by a post-focal transmission valley, suggesting defocusing behaviour (i.e., negative sign NLO refractive index parameter γ').

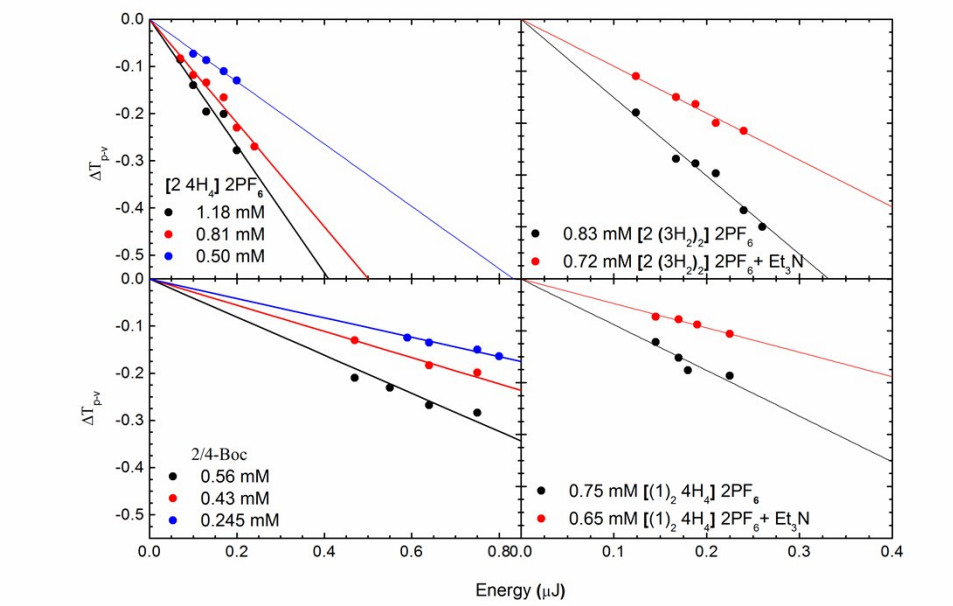

Figure S19. Variation of the ΔT_{p-v} parameter versus the laser energy, under 35 ps, 532 nm laser excitation.

The variation of the ΔT_{p-v} parameter, obtained from the "divided" Z-scans, as a function of the laser energy is presented in Figure S19. As shown, a good linear variation was found to hold in all cases, the straight lines of Fig. S19, corresponding to the best linear fits of the experimental data points. From the slopes of these best fits lines the nonlinear refractive index parameter γ' was determined using equation

(2), while the real part of the third-order susceptibility (Re $\chi^{(3)}$) was then calculated from equation (3). The second hyperpolarizability γ values of all molecular systems studied in this work are reported in Tables S1 and S2, together with the corresponding value for [60]fullerene for comparison purposes.

Table S1. Second hyperpolarizability, γ, values of the [60]fullerene, the **3**- and **4**-BOC, the **3**H_2 and **4**H_4 fullerene based molecular systems, the **1** and **2** porphyrins crown ether complexes, the **1**/**3**-Boc, **2**/**3**-Boc, **1**/**4**-Boc and **2**/**4**-Boc in 1:1 mixtures, and the pseudorotaxanes assemblies [**1**·**3**H_2]·PF_6, [(**1**)$_2$·**4**H_4]·2PF_6, [**2**·(**3**H_2)$_2$]·2PF_6 and [**2**·**4**H_4]·2PF_6, obtained under 35 ps, 532 nm laser excitation.

Entry	Sample	ε@532nm (L mol^{-1}cm^{-1})	Reγ (×10^{-31} esu)	Imγ (×10^{-31} esu)	γ (×10^{-31} esu)
1	C_{60} [5]	811.7	<0.08	0.28±0.01	0.28±0.01
2	**3**-BOC	920	-	0.30±0.02	0.30±0.02
3	**4**-BOC	1054	-	0.35±0.05	0.35±0.05
4	**3H$_2$**	1171	-	0.32±0.05	0.32±0.05
5	**4H$_4$**	1403	-	0.28±0.02	0.28±0.02
6	**1**	3426	-(5.1±0.2)	3.0±0.2	5.9±0.3
7	**2**	3693	-(4.0±0.3)	3.9±0.2	5.6±0.4
8	**1/3**-Boc	4671	-(4.4±0.2)	5.3±0.9	6.8±0.9
9	**2/3**-Boc	4556	-(3.9±0.4)	5.7±0.4	6.9±0.6
10	**1/4**-Boc	4581	-(4.0±0.6)	4.0±0.3	6.0±0.6
11	**2/5**-Boc	4562	-(3.8±0.2)	4.0±1.0	5.4±1.0

As can be seen, the fullerene derivatives **3**- and **4**-Boc, **3**H_2 and **4**H_4 (i.e., entries 2, 3, 4 and 5) exhibited similar NLO response to that of [60]fullerene (i.e., entry 1) [5], having negligible NLO refraction and substantial NLO absorption of

positive sign (i.e., RSA). The two porphyrin crown ether complexes, namely **1** and **2** (i.e., entries 6, 7), were found to exhibit a 20-fold larger NLO response than that of [60]fullerene derivatives, exhibiting both strong NLO absorption and refraction, the latter of negative sign, corresponding to self-defocusing. Then, the **1**/**3**-Boc, the **2**/**3**-Boc, the **1**/**4**-Boc and the **2**/**4**-Boc (i.e., entries 8, 9, 10 and 11) 1:1 mixtures of the [60]fullerene derivatives with the porphyrin crown ether complexes were all found to exhibit very similar NLO response within the experimental uncertainties. In fact, their second hyperpolarizability values were found to be very close to the values of porphyrin crown ether complexes, as the [60]fullerene nonlinearity was much weaker to influence considerably the NLO response of the mixtures. In Table S3 the second hyperpolarizability, γ, values of some other donor-acceptor fullerene derivatives reported in the literature are shown for comparison purposes.

Table S2. Second hyperpolarizability, γ, values of the pseudorotaxanes assemblies in CH_2Cl_2/CH_3CN (9:1 *v/v*, c = 2.5 × 10^{-4} M) solutions, before and after the addition of base (Et_3N). The NLO response of the reference molecules is also included.

Entry	Sample	ε@532nm ($L\ mol^{-1}cm^{-1}$)	Reγ ($\times10^{-31}$ esu)	Imγ ($\times10^{-31}$ esu)	γ ($\times10^{-31}$ esu)
1	**1**	3426	-(5.1±0.2)	3.0±0.2	5.9±0.3
2	**2**	3693	-(4.0±0.3)	3.9±0.2	5.6±0.4
3	**3**H_2·PF_6	1171	-	0.32±0.05	0.32±0.05
4	**4**H_4·2PF_6	1403	-	0.28±0.02	0.28±0.02
5	[**1**·**3**H_2]·PF_6	4740	-(3.3±0.3)	4.4±0.8	5.4±1.0
6	[**1**·**3**H_2]·PF_6+ base	4567	-(3.5±0.3)	2.8±0.9	4.5±0.7
7	[(**1**)$_2$·**4**H_4]·2PF_6	6332	-(4.5±0.1)	4.9±0.2	6.7±0.2
8	[(**1**)$_2$·**4**H_4]·2PF_6 + base	4130	-(3.2±0.1)	3.8±0.4	5.0±0.4
9	[**2**·(**3**H_2)$_2$]·2PF_6	5971	-(8.4±0.9)	7.7±0.8	11.4±1.2
10	[**2**·(**3**H_2)$_2$]·2PF_6 + base	4830	-(5.9±0.1)	2.0±0.3	6.2±0.2
11	[**2**·**4**H_4]·2PF_6	4582	-(6.2±0.6)	4.4±0.7	7.5±0.9
12	[**2**·**4**H_4]·2PF_6 + base	3764	-(2.9±0.1)	2.7±0.6	3.9±0.5

Table S3. Second hyperpolarizability, γ, values of some fullerene derivatives from the literature.

Sample	γ ($\times 10^{-31}$esu)	Ref.
C_{60} derivative 1	1.8±0.8	[9a]
C_{60} derivative 2	3.3±1.0	
C_{60} derivative 3	11.6±0.4	
C_{60} derivative 1A	0.418±0.039	[9b]
C_{60} derivative 1B	0.219±0.064	
C_{60} derivative 2A	0.871±0.062	
C_{60} derivative 2B	0.480±0.080	
TPhA–C_{60} 1	0.26±0.04	[9c]
TPhA–C_{60} 2	0.38±0.09	
TPhA–$(C_{60})_2$ 3	1.72±0.23	
C_{60} derivative ph	0.237	[9d]
C_{60} derivative an	0.202	
[C_{60} derivative 2Q	2.13	[9e]
C_{60} derivative 4Q	1.67	
C_{60} derivative 1	5.93	[9f]
C_{60} derivative 2	4.68	
C_{60} derivative 3	3.86	
C_{60} derivative 4	3.08	
C_{60} derivative 5	3.76	
C_{60} derivative 6	6.07	
$(Ph_3P)_2PtC_{60}$	14.8	[9g]
$((C_5H_5)_2Fe)_2C_{60}$	1.82	

5 S8 Molecular Modelling

The calculations were performed using the Gaussian 09 package [Gaussian 09, Revision A.1, M. J. Frisch, G. W. Trucks, H. B. Schlegel, G. E. Scuseria, M. A. Robb, J. R. Cheeseman, G. Scalmani, V. Barone, B. Mennucci, G. A. Petersson, H. Nakatsuji, M. Caricato, X. Li, H. P. Hratchian, A. F. Izmaylov, J. Bloino, G. Zheng,

J. L. Sonnenberg, M. Hada, M. Ehara, K. Toyota, R. Fukuda, J. Hasegawa, M. Ishida, T. Nakajima, Y. Honda, O. Kitao, H. Nakai, T. Vreven, J. A. Montgomery, Jr., J. E. Peralta, F. Ogliaro, M. Bearpark, J. J. Heyd, E. Brothers, K. N. Kudin, V. N. Staroverov, R. Kobayashi, J. Normand, K. Raghavachari, A. Rendell, J. C. Burant, S. S. Iyengar, J. Tomasi, M. Cossi, N. Rega, J. M. Millam, M. Klene, J. E. Knox, J. B. Cross, V. Bakken, C. Adamo, J. Jaramillo, R. Gomperts, R. E. Stratmann, O. Yazyev, A. J. Austin, R. Cammi, C. Pomelli, J. W. Ochterski, R. L. Martin, K. Morokuma, V. G. Zakrzewski, G. A. Voth, P. Salvador, J. J. Dannenberg, S. Dapprich, A. D. Daniels, Ö. Farkas, J. B. Foresman, J. V. Ortiz, J. Cioslowski, and D. J. Fox, Gaussian, Inc., Wallingford CT, 2009.].

Geometry optimization of porphyrins x and y, fullerenes z and j and the complexes 8, 10 and 12 was carried and the molecular volume was computed. Then the hydrodynamic radius (r) of an ideal sphere including the molecules was also derived. Dealing with such large systems, the semi-empirical method PM6 (Stewart, J. J. P. *Journal of molecular modeling* **2007**, *13*, 1173–213) was chosen as appropriate to obtain qualitative information about these molecules.

Table S4. HOMO and LUMO orbitals for [*n*]pseudorotaxanes.

HOMO	LUMO
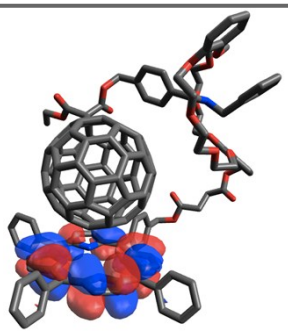	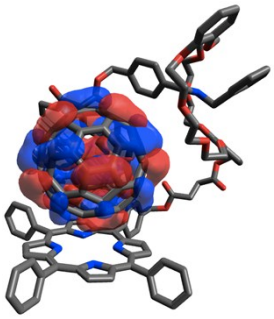
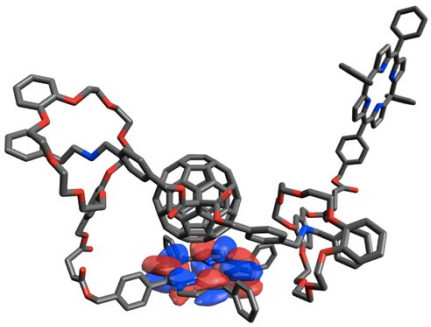	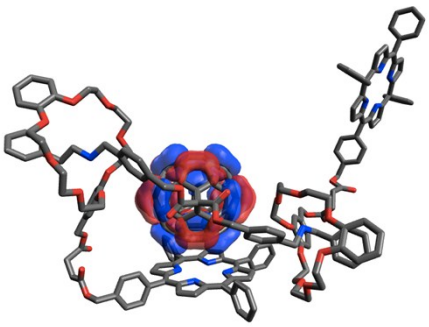
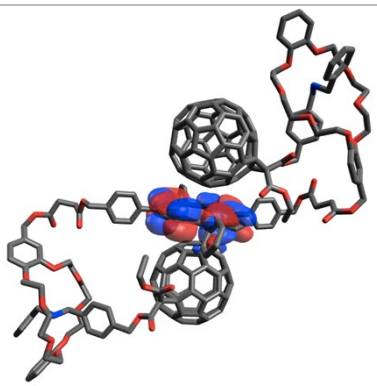	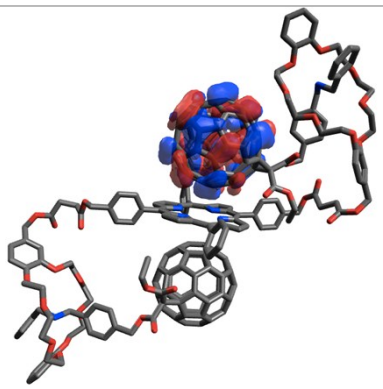
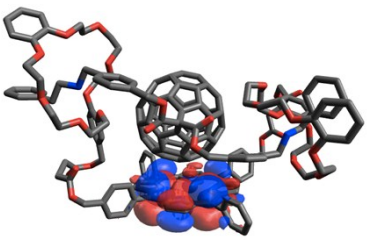	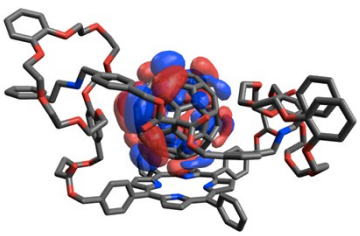

S9 References

[1] G. A. Crosby and J. N. Demas, *J. Phys. Chem.* **1971**, *75*, 991-1024.

[2] K. Nakamaru, *Bull. Chem. Soc. Jpn.* **1982**, *55*, 2697-2705.

[3] F. Diederich, L. Echegoyen, M. Gome-Lopez, R. Kessinger and J. F. Stoddart, *J. Chem. Soc., Perkin Trans.* **1999**, *2*, 1577-1586.

[4] H. W. Gibson, Z. Ge, J. W. Jones, K. Harich, A. Pederson and H. C. Dorn, *J. Polym. Sci. Part A: Polym. Chem.* **2009**, *47*, 6472–6495.

[5] X. Wang, V. Ervithayasuporn, Y. Zhang and Y. Kawakami, *Chem. Commun.* **2011**, *47*, 1282-1284.

[6] B. Ventura, L. Flamigni, G. Marconi, F. Lodato and D. L. Officer, *New J. Chem.* **2008**, *32*, 166-178.

[7] G. Accorsi and N. Armaroli, *J. Phys. Chem. C* **2010**, *114*, 1385-1403.

[8] a) P. Aloukos, G. Chatzikyriakos, I. Papagiannouli, N. Liaros and S. Couris, *Chemical Physics Letters* **2010**, *495*, 245-250; b) N. Liaros, P. Aloukos, A. Kolokithas-Ntoukas, A. Bakandritsos, T. Szabo, R. Zboril and S. Couris, *The Journal of Physical Chemistry C* **2013**, *117*, 6842-6850.

[9] a) E. Xenogiannopoulou, M. Medved, K. Iliopoulos, S. Couris, M. G. Papadopoulos, D. Bonifazi, C. Sooambar, A. Mateo-Alonso, M. Prato, *Chemphyschem* 2007, **8**, 1056-1064; b) A. Mateo-Alonso, K. Iliopoulos, S. Couris, M. Prato, *J. Am. Chem. Soc.* 2008, **130**, 1534-1535; c) R. Zalesny, O. Loboda, K. Iliopoulos, G. Chatzikyriakos, S. Couris, G. Rotas, N. Tagmatarchis, A. Avramopoulos, *Phys Chem. Chem. Phys.* 2010, **12**, 373; d) Y. Cheng, H. Hao, H. Xiao, S. Zhu, *J. Phys. B: At. Mol. Opt. Phys.* 2009, **42**, 235401; e) Y. Cheng, T. He, H. Hao, S. Zhu, H. Xiao, *Optics Communications* 2009, **282**, 4271; f) Y.L. Mao,

Y.G. Cheng, J.H. Liu, B.C. Lin, Y.P. Huo, H.P. Zeng, *Chin. Phys. Lett.* 2007, **24**, 950; g) O. B. Mavritsky, A.N. Egorov, A.N. Petrovsky, K.V. Yakubovsky, W.J. Blau, D.N. Weldon, F.Z. Henary, *Proc. SPIE* 1996, **2854**, 254.

5